Gracheva et al., http://www.jcb.org/cgi/content/full/jcb.201506099/DC1

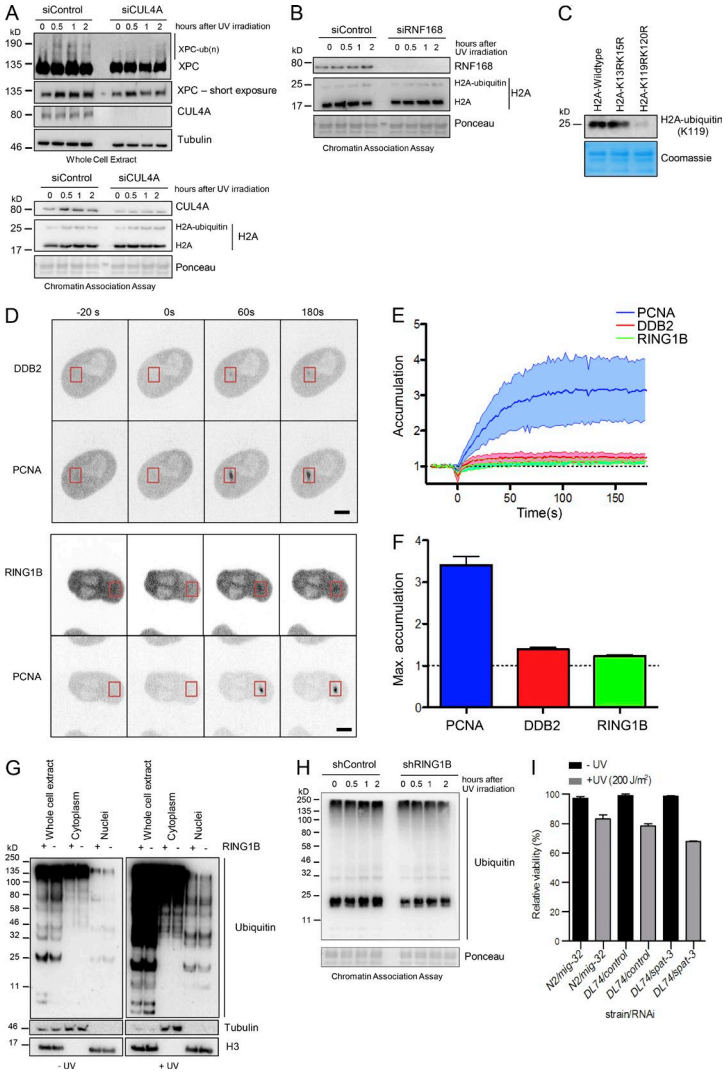

Figure S1. **Function of RING1B in H2A ubiquitylation during UV-triggered DNA repair.** (A) Depletion of CUL4A has no impact on H2A ubiquitylation but reduces XPC ubiquitylation. (top) Whole-cell extracts of HEK293T cells treated with siRNA (control, *CUL4A*) were prepared at the stated time points after UV irradiation, subjected to Western blotting and probed with the indicated antibodies. (bottom) Chromatin association assays of UV irradiated HEK293T cells treated with siRNAs (control, *CUL4A*). De–cross-linked material of the respective time points was subjected to Western blotting and probed with the indicated antibodies. (B) Depletion of RNF168 has no impact on H2A ubiquitylation after UV irradiation at 10 J/m^2. Chromatin association assays of UV-irradiated HEK293T cells treated with siRNAs (control, *RNF168*). De–cross-linked material of the respective time points was subjected to Western blotting and probed with the indicated antibodies. (C) Verification of H2A-ubiquitin antibodies used in this study (H2A-K119-ubiquitin; Cell Signaling Technology). The antibody specifically recognizes monoubiquitylation of histone H2A at lysine 119. HEK293T cells were transfected with ^{FLAG}H2A, ^{FLAG}H2A-K13R-K15R, and ^{FLAG}H2A-K119R-K120R. Mononucleosomes were purified after sonification and purification with FLAG-M2-agarose beads. Purified material was subjected to Western blotting and blots were incubated with H2A-ubiquitin antibodies. The integrity of nucleosomes was visualized by Coomassie staining. (D) DDB2 and RING1B accumulate at sites of DNA damage. Time-lapse microscopy of a midnuclear section before (−20 s) directly after (0 s) and 60 and 180 s after DNA damage was inflicted in a spot by application of 1 mJ focused (1-µm) 405-nm laser microirradiation. The location of the microirradiation is highlighted with a red square. DDB2-GFP and RING1B-YFP were transfected into HeLa-Kyoto cells stably expressing Cherry-PCNA as a marker for DNA damage. Bar, 5 µm. (E) DDB2 and RING1B accumulate at sites of DNA damage inflicted by irradiation with a 405-nm laser. DDB2-GFP and RING1B-YFP were transfected into HeLa-Kyoto cells stably expressing Cherry-PCNA as a marker for DNA damage. Accumulation of PCNA (blue), DDB2 (red), and RING1B (green) was measured in at least 10 cells each and the mean accumulation is plotted together with the SD (shaded areas). The dotted line shows the baseline for accumulation at 1. (F) The maximum accumulation for each protein is represented as a barplot reflecting the mean and SD measured in the individual cells. (G) Depletion of RING1B does not affect cellular ubiquitylation events. Fractionation of protein extracts from control and RING1B knockdown HEK293T cells before or after UV irradiation. Fractions (whole-cell extract, cytoplasm, and nuclei) were subjected to Western blotting and probed with the indicated antibodies. (H) Depletion of RING1B does not interfere with ubiquitylation events at chromatin. Chromatin association assays of control and RING1B knockdown HEK293T cell lines after UV irradiation. De–cross-linked material of the respective time points was subjected to Western blotting and probed with ubiquitin antibody. (I) Epistatic relationship of *mig-32* and *spat-3*. Wild-type nematodes (N2) or *mig-32* mutants (DL74) were fed with either control or *spat-3* RNAi–producing bacteria. The relative viability was analyzed after UV irradiation (200 J/m^2). Values are given as mean ± SEM (n = 2).

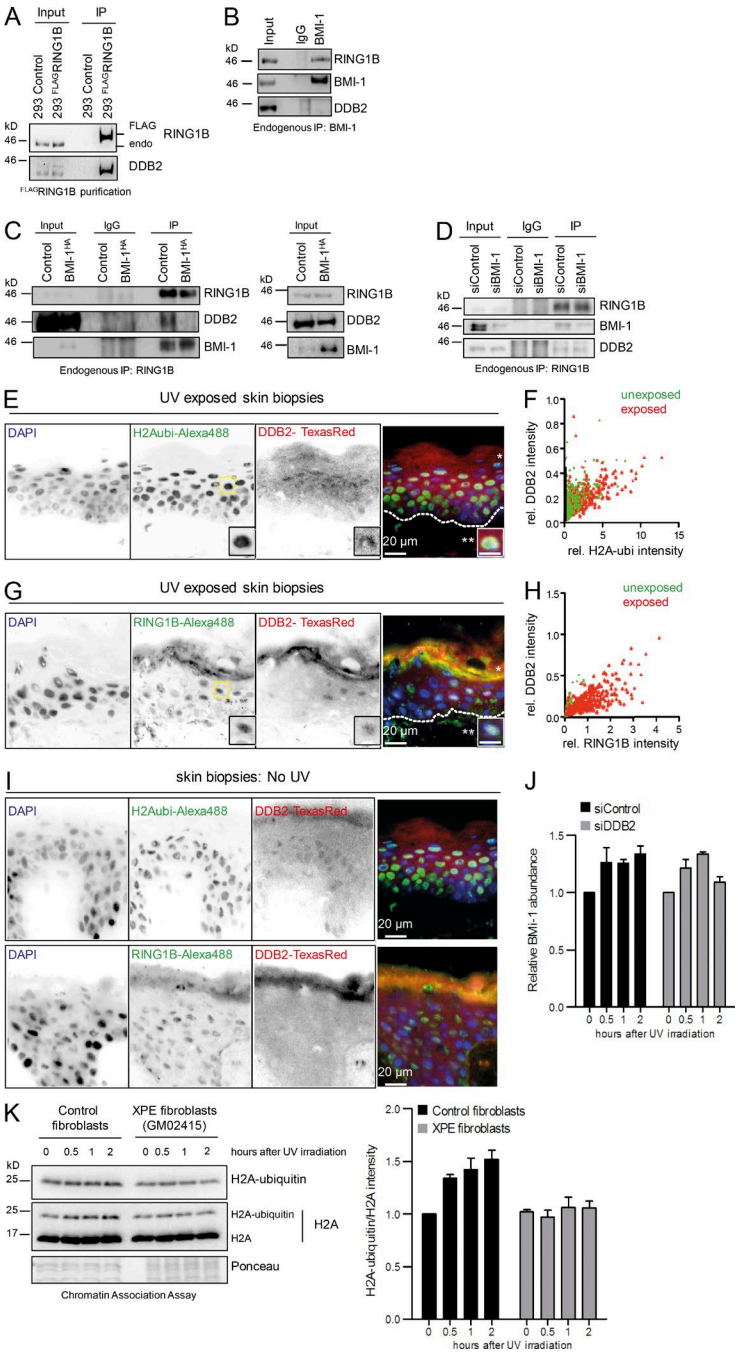

Figure S2. **Functional analysis of RING1B and DDB2 in UV-triggered DNA repair.** (A) RING1B binds DDB2. Immunoprecipitations from HEK293T cell lines stably expressing ^{FLAG}RING1B. Precipitated material was subjected to Western blotting and probed with the indicated antibodies. Inputs correspond to 3%. (B) BMI-1 does not interact with DDB2 after UV irradiation. Endogenous immunoprecipitations with BMI-1 antibodies. Western blots of the precipitated material were incubated with the indicated antibodies. Inputs correspond to 3%. (C) BMI-1 and DDB2 compete for binding to RING1B. Endogenous immunoprecipitations with RING1B antibodies were performed after overexpressing BMI-1^{HA} or empty vector (control) and after UV irradiation. Precipitated material was subjected to Western blotting and probed with the indicated antibodies. Inputs correspond to 3%. (D) Depletion of BMI-1 does not interfere with RING1B-DDB2 interaction. Endogenous immunoprecipitations with RING1B antibodies were performed after treating cells with siRNA (control, *BMI-1*) and after UV irradiation. Precipitated material was subjected to Western blotting and probed with the indicated antibodies. Inputs correspond to 3%. (E) H2A-ubiquitin colocalizes with DDB2 in UV-exposed skin sections. Cryosections of UV-exposed skin were stained with H2A ubiquitin (green) and DDB2 (red) antibodies. Dotted line, stratum basale; *, stratum corneum; **, dermis. Bars: 20 µm; (inset) 10 µm. (F) Correlation of H2A ubiquitin and DDB2 by single-cell analysis. (G) RING1B colocalizes with DDB2 in UV-exposed skin sections. Cryosections of UV-exposed skin were stained with RING1B (green) and DDB2 (red) antibodies. Dotted line, stratum basale; *, stratum corneum; **, dermis. Bar: 20 µm; (inset) 10 µm. (H) Correlation of RING1B and DDB2 by single-cell analysis. All intensities are normalized to the DNA content of the corresponding nucleus for UV and non-UV conditions (Fig. S2 I). At least 200 nuclei were analyzed in at least three sections. (I) Stainings of skin biopsies without UV treatment. Related to Fig. S2 (E and G). Cryosections of non-exposed skin were stained with the indicated antibodies. (J) Corresponding to Fig. 2 F. The relative BMI-1 abundance was calculated. Values are given as mean ± SEM (n = 3). (K) Chromatin association assays in control fibroblasts and XPE (DDB2) fibroblasts (GM02415) after UV irradiation. De–cross-linked material of the respective time points was subjected to Western blotting and probed with the indicated antibodies. H2A-ubiquitin levels were calculated. Values are given as mean ± SEM (n = 3).

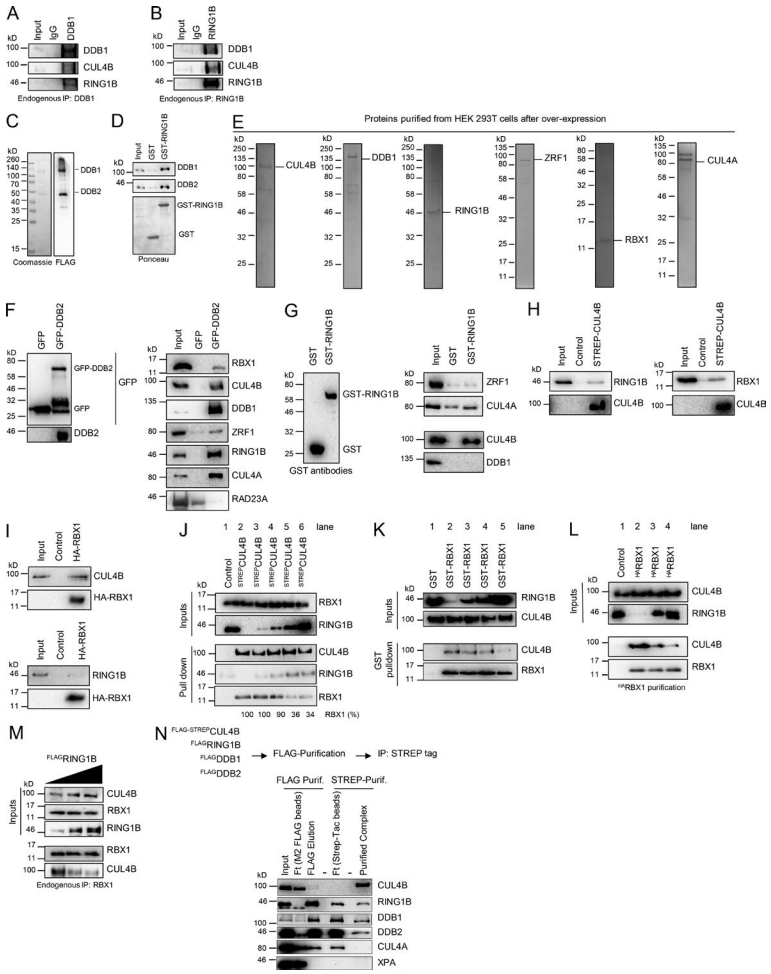

Figure S3. **RING1B forms a stable complex with DDB1, DDB2, and CUL4B.** (A) Endogenous immunoprecipitations with DDB1 antibodies. Precipitated material was subjected to Western blotting and probed with the indicated antibodies. Inputs correspond to 3%. (B) Endogenous immunoprecipitations with RING1B antibodies. Precipitated material was subjected to Western blotting and probed with the indicated antibodies. Inputs correspond to 3%. (C) Purification of DDB1–DDB2 protein complexes. After simultaneous overexpression of both proteins (^{FLAG}DDB1 and ^{FLAG}DDB2) in HEK293T cells, purifications were performed using FLAG-M2-agarose. Purified material was subjected to Western blotting and probed with the indicated antibodies and colloidal Coomassie staining. (D) GST pull-down with the purified DDB1–DDB2 complexes (S3C) using recombinant GST and GST-RING1B proteins. Precipitated material was subjected to Western blotting and probed with the indicated antibodies. (E) Purity of proteins used for the in vitro experiments. Proteins were overexpressed in HEK293T cells by transfection of the following individual plasmids ($^{FLAG\text{-}STREP}$CUL4B, ^{FLAG}DDB1, ^{FLAG}RING1B, ^{FLAG}ZRF1, ^{FLAG}ZRF1, ^{HA}RBX1, and ^{HA}CUL4A), purified to near homogeneity via the respective epitope tag and analyzed in a polyacrylamide gel with subsequent Coomassie staining. (F) Interaction partners of DDB2 based on in vitro pull-downs. GFP or GFP-DDB2 were immobilized on beads (left) and incubated with the indicated purified proteins. The precipitated material was subjected to Western blotting and blots were incubated with the indicated antibodies (right). Inputs correspond to 10%. (G) RING1B interacts directly with CUL4B, but not with DDB1, in vitro. GST or GST-RING1B was immobilized on beads (left) and incubated with the stated purified proteins. The precipitated material was subjected to Western blotting, and blots were incubated with the indicated antibodies (right panel). Inputs correspond to 10%. (H) CUL4B interacts with RING1B and RBX1 in vitro. $^{FLAG\text{-}STREP}$CUL4B was immobilized on beads and incubated with the indicated purified proteins. Empty beads were used as control. The precipitated material was subjected to Western blotting and blots were incubated with the indicated antibodies. Inputs correspond to 10%. (I) RBX1 interacts with CUL4A, but not RING1B, in vitro. ^{HA}RBX1 was immobilized on beads and incubated with the indicated purified proteins. Empty beads were used as control. The precipitated material was subjected to Western blotting and blots were incubated with the indicated antibodies. Inputs correspond to 10%. (J) RING1B and RBX1 compete for binding to CUL4B. $^{FLAG\text{-}STREP}$CUL4B immobilized on beads and empty beads (Control) were incubated with constant amounts of purified RBX1 and increasing amounts of RING1B. RING1B levels were doubled stepwise reaching an eightfold molar excess of RING1B over the other components (relative molarity RING1B: RBX1; lane 3, 1:1; lane 4, 2:1; lane 5, 4:1; lane 6, 8:1). Precipitated material was subjected to Western blotting and blots were incubated with the indicated antibodies. Inputs correspond to 10%. (K) RING1B and RBX1 compete for binding to CUL4B. GST and GST-RBX1 immobilized on beads were incubated with constant amounts of purified CUL4B and RBX1 and increasing amounts of RING1B. RING1B levels were doubled stepwise reaching an eightfold molar excess of RING1B over the other components (relative molarity RING1B: RBX1/CUL4B; lane 2, 1:1; lane 3, 2:1; lane 4, 4:1; lane 5, 8:1). Control beads were incubated with CUL4B and maximum amounts of RING1B. Precipitated material was subjected to Western blotting, and blots were incubated with the indicated antibodies. Inputs correspond to 10%. (L) RING1B competes with RBX1 for binding to CUL4B. ^{HA}RBX1 was immobilized on beads and incubated with constant amounts of CUL4B and RBX1 and increasing amounts of RING1B (relative molarity RING1B: RBX1/CUL4B; lane 3, 5:1; lane 4 10:1). Control beads were incubated with CUL4B and the maximum amounts of RING1B (10×). The precipitated material was subjected to Western blotting, and blots were incubated with the indicated antibodies. Inputs correspond to 10%. (M) HEK293T cells expressing increasing amounts of ^{FLAG}RING1B construct were UV irradiated. After immunoprecipitation with RBX1 antibodies, the precipitated material was subjected to Western blotting and blots were incubated with the indicated antibodies. Inputs correspond to 5%. (N) Purification scheme for the assembly of DDB1-DDB2-RING1B-CUL4B (UV-RING1B) complexes in vivo. The relevant proteins with FLAG or FLAG-STREP tags were coexpressed in HEK293T cells (top). Cells were not irradiated with UV light. After sequential purifications with FLAG-M2-agarose and STREP-Tactin beads, input, flow-through (Ft), and eluate fractions were subjected to Western blotting and probed with the indicated antibodies.

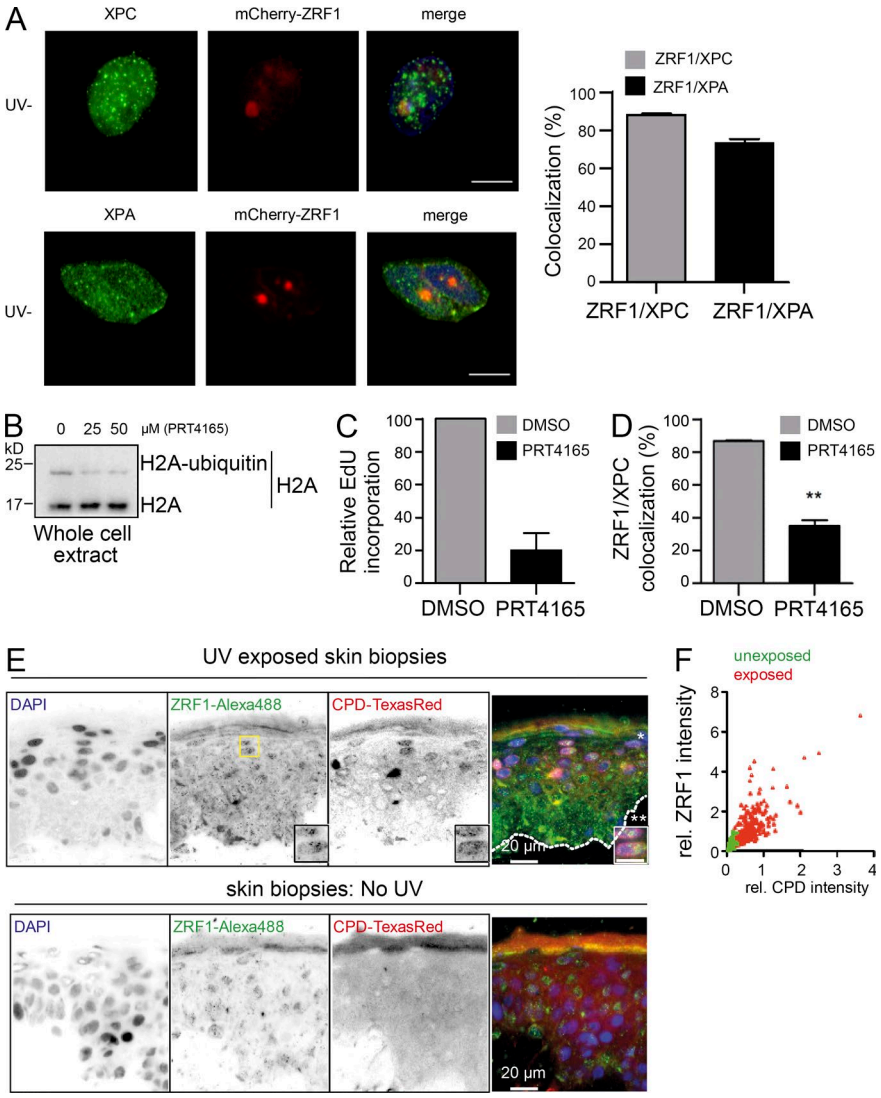

Figure S4. **Function of ZRF1 in UV-triggered DNA repair.** (A) Corresponding to Fig. 4 (C and D). (left) Distribution of XPC and XPA and mCherry-ZRF1 in MRC5 fibroblasts without UV irradiation. Bar, 10 µm. (right) Quantification of ZRF1/XPC and ZRF1/XPA colocalization after UV irradiation. Values are given as mean ± SEM. Data were acquired from three independent experiments (at least 50 nuclei per sample). (B) The RING1B inhibitor PRT4165 reduces H2A ubiquitylation. MRC5 fibroblasts were treated with the indicated doses of PRT4165 for 30 min. Cell extracts were subjected to Western blotting and probed with H2A antibody. (C) PRT4165 reduces unscheduled DNA synthesis after UV irradiation. UDS determined by EdU incorporation in MRC5 fibroblasts after PRT4165 treatment (50 µM, 30 min). Data were acquired from three independent experiments (70–100 nuclei per sample). (D) Quantification of the ZRF1/XPC colocalization after PRT4165 treatment and UV irradiation through a micropore membrane. Values are given as mean ± SEM. Data were acquired from 3 independent experiments (at least 50 nuclei per sample). Significant differences are based on an unpaired two-tailed Student's *t* test, $P < 0.01$. (E) ZRF1 localizes to CPDs in UV exposed skin sections. Cryosections of UV exposed skin were stained with CPD (red) and ZRF1 (green) antibodies. Dotted line, stratum basale; *, stratum corneum; **, dermis. Control stainings of skin biopsy specimens without UV treatment were performed with the same antibodies. Bars: 20 µm; (inset) 10 µm. (F) Correlation of ZRF1 and CPDs by single-cell analysis.

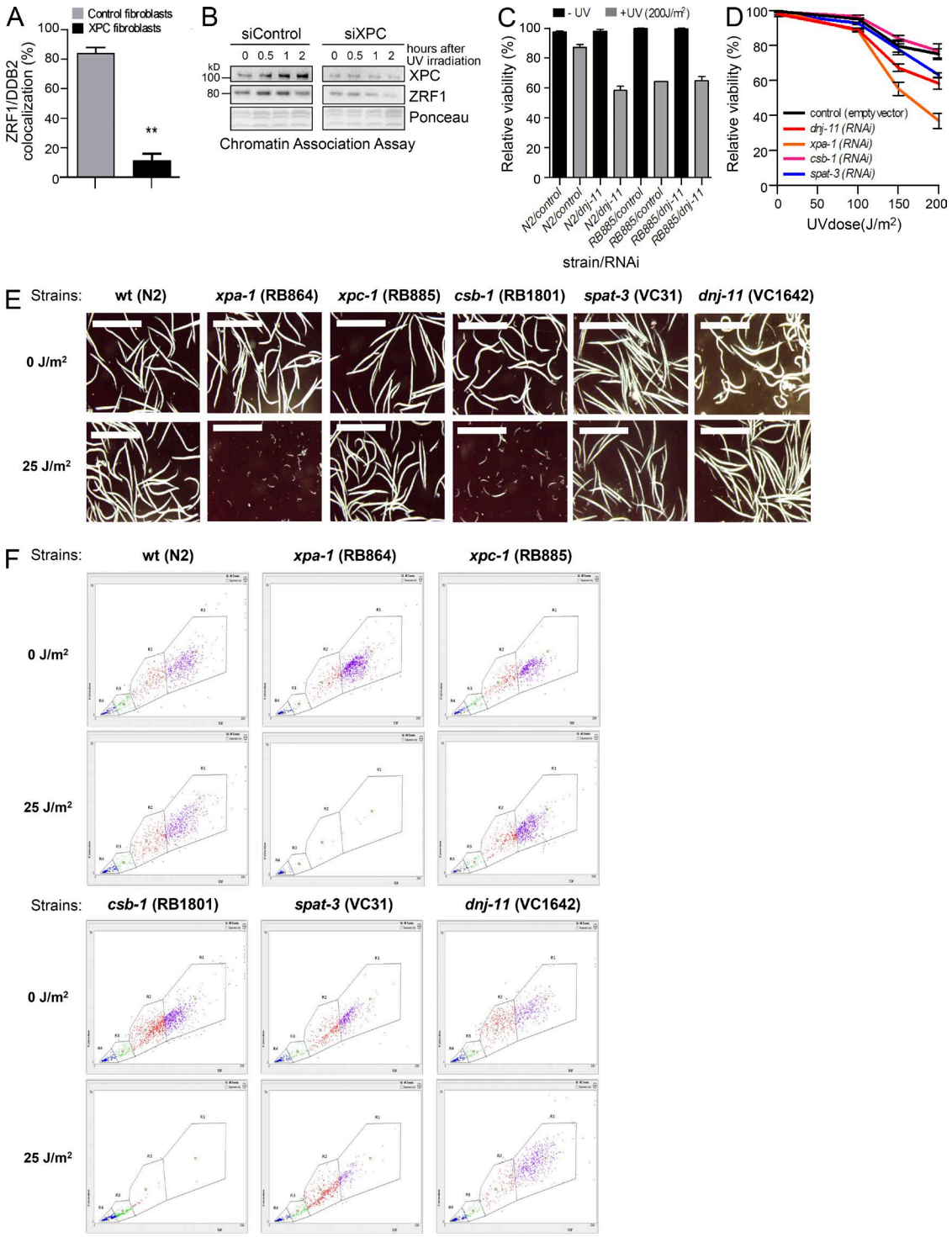

Figure S5. **Function of ZRF1 and RING1B in GG-NER.** (A) Quantification of ZRF1/DDB2 colocalization in control and XPC patient fibroblasts after UV irradiation. Values are given as mean ± SEM. Data were acquired from three independent experiments (at least 40 nuclei per sample). Significant differences are based on an unpaired two-tailed Student's *t* test, $P < 0.01$. (B) ZRF1 depends on XPC to associate with chromatin after UV irradiation. Chromatin association assays of UV-irradiated HEK293T cells treated with siRNAs (control, *XPC*). De-cross-linked material of the respective time points was subjected to Western blotting and probed with the indicated antibodies. (C) Epistatic relationship of *xpc-1* and *dnj-11*. Wild-type nematodes (N2) or *xpc-1* mutants (RB885) were fed with either control or *dnj-11* RNAi–producing bacteria. The relative viability was analyzed after UV irradiation (200 J/m^2). Values are given as mean ± SEM ($n = 4$). (D) Knockdown of *dnj-11* and of *spat-3* leads to an increased UV sensitivity in *C. elegans*. Gene knockdown was mediated via feeding of RNAi-producing bacteria. Late-L4 larval worms were irradiated with UV light at different doses and the relative viability was determined by comparing hatched versus dead embryos (unhatched eggs). Values are given as mean ± SEM ($n = 4$). (E) *C. elegans* knockout mutants for *dnj-11* and *spat-3* show only weak developmental arrest upon somatic UV irradiation. L1 larval worms were UV treated at different doses and imaged after 60 h, when control worms were fully fertile. Bar, 1 mm. (F) Dot blots of *C. elegans* developmental arrest assay. Worm developmental stages were sorted with a large particle sorter (BioSorter; Union Biometrica). During each run, ~1,000 animals were scored according to their extinction and their time of flight (TOF). Clouds were assigned to different *C. elegans* developmental stages as indicated in the graph (R1, L4 stage /adults; R2, L3 stage; R3, L2 stage; R4, L1 stage).

Table S1. **Data summary of developmental arrest assay in mutant strains**

Strain	UV dose (J/m²)	Events in region					Percentage of total in region				
		All	R1	R2	R3	R4	All	R1	R2	R3	R4
wt (N2)	0	1,009	494	181	92	159	100	48.96	17.94	9.12	15.76
wt (N2)	25	1,013	526	210	44	191	100	51.93	20.73	4.34	18.86
wt (N2)	50	1,012	43	310	391	245	100	4.25	30.63	38.64	24.21
wt (N2)	75	1,014	4	24	459	524	100	0.39	2.37	45.27	51.68
wt (N2)	100	1,007	0	2	19	982	100	0.00	0.20	1.89	97.52
xpa-1 (RB864)	0	1,346	918	145	20	243	100	68.20	10.77	1.49	18.05
xpa-1 (RB864)	25	1,165	6	2	5	1147	100	0.52	0.17	0.43	98.46
xpa-1 (RB864)	50	1,008	1	0	5	995	100	0.10	0.00	0.50	98.71
xpa-1 (RB864)	75	1,015	1	1	6	997	100	0.10	0.10	0.59	98.23
xpa-1 (RB864)	100	1,013	1	3	5	1000	100	0.10	0.30	0.49	98.72
xpc-1 (RB885)	0	885	482	194	69	135	100	54.46	21.92	7.80	15.25
xpc-1 (RB885)	25	1,003	643	226	47	66	100	64.11	22.53	4.69	6.58
xpc-1 (RB885)	50	1,019	319	453	134	100	100	31.01	44.46	13.15	9.81
xpc-1 (RB885)	75	1,011	2	44	421	536	100	0.20	4.35	41.64	53.02
xpc-1 (RB885)	100	1,013	2	2	257	741	100	0.20	0.20	25.37	73.15
csb-1 (RB1801)	0	1,703	625	566	103	355	100	36.70	33.24	6.05	20.85
csb-1 (RB1801)	25	1,251	1	24	344	877	100	0.08	1.92	27.50	70.10
csb-1 (RB1801)	50	1,028	1	0	27	987	100	0.10	0.00	2.63	96.01
csb-1 (RB1801)	75	1,030	1	1	4	1019	100	0.10	0.10	0.39	98.93
csb-1 (RB1801)	100	1,024	0	0	1	1017	100	0.00	0.00	0.10	99.32
spat-3 (VC31)	0	1,002	338	230	53	311	100	33.73	22.95	5.29	31.04
spat-3 (VC31)	25	1,005	145	380	109	309	100	14.43	37.81	10.85	30.75
spat-3 (VC31)	50	1,005	16	217	247	474	100	1.59	21.59	24.58	47.16
spat-3 (VC31)	75	1,003	0	0	56	935	100	0.00	0.00	5.58	93.22
spat-3 (VC31)	100	1,025	0	0	16	981	100	0.00	0.00	1.56	95.71
dnj-11 (VC1642)	0	1,051	335	306	59	266	100	31.87	29.12	5.61	25.31
dnj-11 (VC1642)	25	1,080	530	127	56	276	100	49.07	11.76	5.19	25.56
dnj-11 (VC1642)	50	1,034	57	474	140	294	100	5.51	45.84	13.54	28.43
dnj-11 (VC1642)	75	1,039	3	10	307	682	100	0.29	0.96	29.55	65.64
dnj-11 (VC1642)	100	1,075	2	0	42	998	100	0.19	0.00	3.91	92.84

Raw data underlying Fig. S6 I. Worm developmental stages were sored sorted with a large-particle sorter (BioSorter; Union Biometrica). During each run, ~1,000 animals were scored according to their extinction and their time of flight. Regions were assigned to different *C. elegans* developmental stages as indicated in Fig. S6 J.

Table S2. **Plasmids used in this study**

Plasmids	Source
pCMV2-FLAG-H2A	Richly et al. (2010)
pCMV2-FLAG-H2A-K119RK120R	Richly et al. (2010)
pcDNA3.1-FLAG-H2AK13-15R	Gift from the Sixma laboratory (Netherlands Cancer Institute, Amsterdam, Netherlands)
RING1B-YFP	Gift from the di Croce laboratory (Centre for Genomic Regulation, Barcelona, Spain)
pCMV2-FLAG-RING1B	Richly et al. (2010)
pCMV-TAG2b	Sigma-Aldrich
pT3-EF1a-BMI1	Addgene (31783)
pDNA3-FLAG-DDB2	Gift from the Tanaka laboratory (Osaka University, Osaka, Japan)
pGEX-UbcH5	Gift from the Rape laboratory (University of California, Berkeley, Berkeley, CA)
pET-UBA1	Gift from the Rape laboratory
pGEX-RING1B	Richly laboratory
pEGFP-C1-DDB2	Gift from the Dantuma laboratory (Karolinska University, Solna, Sweden)
pcDNA3-FLAG-DDB1	Addgene (19918)
pcDNA-FLAG-STREP-CUL4B	Gift from the Beli laboratory (Institute of Molecular Biology, Mainz, Germany)
pcDNA3-HA-RBX1	Addgene (19897)
pcDNA3-HA-CUL4A	Addgene (19907)
mCherry-ZRF1	Richly laboratory
pCMV2-FLAG-H2AX	Richly laboratory
pCMV2-FLAG-ZRF1	Richly et al. (2010)
pET-HIS-ZRF1	Richly et al. (2010)
HIS-HA-GFP-XPC	Gift from the Cardoso laboratory (Technische Universität Darmstadt, Germany)
pMT125-HA-Ubiquitn	Richly laboratory
pCS2-HIS-Ubiquitin-WT	Gift from the Rape laboratory

Table S3. **shRNA and siRNA sequences used for this study**

Gene	TRC code	Sequence
shRNA		
NMC	TRC1/1.5	5′-CCGGCAACAAGATGAAGAGCACCAACTCGAGTTGGTGCTCTTCATCTTGTTGTTTTT-3′
DDB2	TRCN0000083995	5′-CCGGGCTGAAGTTTAACCCTCTCAACTCGAGTTGAGAGGGTTAAACTTCAGCTTTTTG-3′
ZRF1	TRCN0000254058	5′-CCGGCTGGAAGAACCAAGATCATTACTCGAGTAATGATCTTGGTTCTTCCAGTTTTTG-3′
RING1B	TRCN0000033697	5′-CCGGGCCAGGATCAACAAGCACAATCTCGAGATTGTGCTTGTTGATCCTGGCTTTTTG-3′
XPC	TRCN0000307193	5′-CCGGGCAACAGCAAAGGGAAAGAAACTCGAGTTTCTTTCCCTTTGCTGTTGCTTTTTG-3′
siRNA		
Gene	siRNA source	Oligo name, sequence
Negative control	Sigma-Aldrich	SIC001. (Sequence not disclosed by the company)
DDB2	Sigma-Aldrich	SASI_Hs01_00101645. (Sequence not disclosed by the company)
		SASI_Hs01_00101647. (Sequence not disclosed by the company)
DDB2	GE Healthcare	D-011-22-01. 5′-CAACUAGGCUGCAAGACUU-3′
		D-011-22-02. 5′-GAUAUCAUGCUCUGGAAUU-3′
		D-011-22-03. 5′-GACCUCCGAGAUUGUAUUA-3′
		D-011-22-04. 5′-AGAGCGAGAUCCGAGUUUA-3′
RNF168	GE Healthcare	D-0071520-18. 5′-GAGUAUCACUUACGCGCUA-3′
		D-0071520-03. 5′-AGAAGGAGGUGGAUAAAGA-3′
		D-0071520-02. 5′-GAAAUUCUCUCGUCAACGU-3′
		D-0071520-01. 5′-GGAAGUGGCUGAUGACUAU-3′
CUL4A	Sigma-Aldrich	EHU020361. (Sequence not disclosed by the company)
BMI1	Sigma-Aldrich	EHU004421. (Sequence not disclosed by the company)
CUL4B	Sigma-Aldrich	EHU064911. (Sequence not disclosed by the company)
XPC	Sigma-Aldrich	SASI_Hs01_00086530. (Sequence not disclosed by the company)
		SASI_Hs01_00086531. (Sequence not disclosed by the company)

Table S4. **Antibodies used in this study**

Antibody	Source
Histone H2A	Rabbit, ab18255; Abcam
H2A-Ubiquitin (H2A-K119-ubiquitin) clone (D27C4)	Rabbit, # 8240; Cell Signaling Technology
RING1B	Rabbit; self-made (Richly et al., 2010)
RING1B clone (D22F2)	Rabbit, #5694; Cell Signaling Technology
CUL4A	Rabbit, #2699; Cell Signaling Technology
XPC (clone [3.26])	Mouse, ab6264; Abcam
XPC (clone D1M5Y)	Rabbit, #14768; Cell Signaling Technology
RNF168 (clone B-11)	Mouse, sc-101125; Santa Cruz Biotechnology, Inc
BMI-1 (clone D20B7)	Rabbit, #6964; Cell Signaling Technology
Ubiquitin (clone P4D1)	Mouse, #3936; Cell Signaling Technology
αTubulin	Mouse, GT114; GeneTEX
DDB2 (clone D4C4)	Rabbit, #5416; Cell Signaling Technology
DDB2 (clone [2246C4a])	Mouse, ab51017; Abcam
DDB1	Rabbit, A300-462A; Bethyl Laboratories, Inc.
XPA	Mouse, 25500002; Novus Biologicals
XPF (clone 3F2/3)	Mouse, sc-398032; Santa Cruz Biotechnology, Inc
CUL4B	Rabbit, HPA011880; Atlas Antibodies
RBX-1 (clone D3J5I)	Rabbit, #11922; Cell Signaling Technology, Inc.
RAD23A (clone [EPR4818])	Mouse, ab108592; Abcam
FLAG-tag (clone M2)	Mouse, F3165; Sigma-Aldrich
HA-tag (clone Y-11)	Rabbit, sc-805; Santa Cruz Biotechnology, Inc.
HIS-tag	Rabbit, #2365; Cell Signaling Technology
GST	Rabbit, #2622; Cell Signaling Technology
GFP (clone 7.1 and 13.1)	Mouse; Roche
ZRF1	Rabbit; self-made (Richly et al., 2010)
XPD (clone 184.7)	Mouse, sc-101174; Santa Cruz Biotechnology, Inc.
CPD (clone TDM-2)	Mouse; Cosmo Bio
H3	Rabbit, ab1791; Abcam

Provided online are Tables S5 and S6, showing peptide numbers and protein names for all proteins identified in the mass spectrometry analysis after sequential immunoprecipitations with FLAG and RING1B antibodies and of the purified UV–RING1B complex.

References

Richly, H., L. Rocha-Viegas, J.D. Ribeiro, S. Demajo, G. Gundem, N. Lopez-Bigas, T. Nakagawa, S. Rospert, T. Ito, and L. Di Croce. 2010. Transcriptional activation of polycomb-repressed genes by ZRF1. *Nature.* 468:1124–1128. http://dx.doi.org/10.1038/nature09574